

The Chiral Phase Transition and Instanton–Anti-instanton Molecules

T. Schäfer*, E.V. Shuryak and J.J.M. Verbaarschot

Department of Physics

State University of New York at Stony Brook

Stony Brook, New York 11794, USA

Abstract

In this paper we explore the idea that the chiral phase transition in QCD can be described as a transition from a disordered instanton liquid to a strongly correlated phase of polarized instanton anti-instanton molecules. We calculate the degree of polarization of the molecules as a function of the temperature and show that the resulting T -dependence of the fermion determinant drives the chiral phase transition. We also show how the polarization of the molecules can lead to a non trivial behavior of the energy density and pressure. Finally, we study the effect of the presence of molecules on the propagation of quarks at $T \sim T_c$. We derive the corresponding effective interaction and find that the strength in the scalar-pseudoscalar channel is four times the strength in the vector-axial-vector channel which agrees with recent lattice QCD simulations. We give results for the quark condensates as well as mesonic and baryonic correlation functions and find that the 'screening masses' of chiral partners become equal for $T > T_c$, where we still observe substantial attraction in the scalar-pseudoscalar meson channels.

SUNY-NTG-94-24

May 1994

*supported in part by the Alexander von Humboldt foundation.

1 Introduction

Since the first suggestion (see [1] and references therein) that instantons are related to the breakdown of chiral symmetry in the QCD vacuum, significant efforts were made [2, 3, 4, 5] to transform this idea into a quantitative argument.

Recently, two results have led to significant progress in connection with these efforts. First, it was shown [6, 7] that even the simplest possible instanton-based model of the QCD vacuum, the so called Random Instanton Liquid Model (RILM), predicts correlation functions which agree both with phenomenological information (see the recent review [8]) and lattice calculations [9]. In particular, it was shown that many hadrons (including, e.g. pions and nucleons) are bound by the instanton-induced interactions, and that their properties (masses, coupling constants and wave functions) are reproduced by the model.

Secondly, important new results were obtained from the study of 'cooled' lattice configurations. 'Cooling' is a procedure that relaxes any given gauge field configuration to the closest 'classical component' of the QCD vacuum. As emphasized in earlier works, the resulting configurations were found to be of multi-instanton type [10]. The recent work by Chu et al. [11] now concludes that the typical instanton separation is given by $R \simeq 1.1$ fm while the typical size is about $\rho \simeq 0.35$ fm. These numbers essentially reproduce the key parameters of the 'instanton liquid' picture of the QCD vacuum, originally suggested on purely phenomenological grounds [2].

In addition to that, it was found that correlation functions as well as hadronic wave functions in most channels remain practically unchanged after 'cooling'. This confirms that the agreement of previous lattice calculations with the instanton model was not accidental. In fact, these works provide a decisive experiment as far as the validity of the instanton model is concerned, demonstrating that even after eliminating such QCD phenomena as the perturbative gluon exchange and confinement, one still observes hadronic bound states. Moreover, the corresponding masses and wave functions appear to be only mildly affected!

Although many details remain to be worked out, it seems fair to say that instantons

are indeed a major component of the QCD vacuum, producing the quark condensate, the low lying hadronic states and many other nonperturbative features of QCD.

In this paper we discuss properties of the instanton ensemble at finite temperature. Our focus is especially on the region around the chiral phase transition $T \simeq T_c$. The first attempt to understand this phase transition as a rearrangement of the instanton liquid, going from a random phase at low temperatures to a strongly correlated 'molecular' phase at high temperatures was made in [12]. The essential point is that while individual instantons are strongly suppressed in the chirally restored phase (because of the corresponding zero modes), instanton–anti-instanton ($I\bar{I}$) pairs have a finite probability even above T_c . This idea was recently reexamined in [13], and although the basic ingredients of the model are the same, the two works suggest significantly different scenarios for the chiral phase transition.

According to the original idea, chiral symmetry is restored because most of the instantons are removed by a finite temperature instanton suppression factor [14, 15]. This factor describes the effect of Debye screening on the fluctuations around the instanton solution. Of course, it also affects the high temperature molecular phase and allows only a small number of molecules above T_c . In the more recent work [13], on the contrary, it was argued that screening should not be a dominant effect at temperatures below or just above T_c (see also [16]). Instead, it was shown that the temperature dependence of the fermion determinant can provide chiral restoration even without any additional suppression factors¹. This means that one may have a significant number of instantons even above T_c , and that the cause of the phase transition is not the suppression of instantons but a rearrangement of the instanton liquid.

This new scenario for the chiral phase transition implies a number of nonperturbative effects in the region just above T_c . One of these effects was already mentioned in [13]: instantons can provide a substantial contribution to the energy density and pressure even above the chiral phase transition. In this paper, we want to study the effects of

¹In earlier works on the subject [12, 17, 18] the high temperature instanton suppression factor was extrapolated to all temperatures.

the rearrangement of the instanton vacuum in more detail. In particular, we consider the behavior of condensates and hadronic correlation functions through the chiral phase transition. For this purpose we consider a schematic model in which the instanton liquid is described as a mixture of a random and a molecular component. The phase transition is then studied as a function of the fraction of correlated instantons.

The paper is organized as follows. In section 2 we give a general discussion on correlations in the instanton liquid and introduce the concept of instanton–anti-instanton molecules. In section 3 we study the phenomenon of polarization of molecules at finite temperature and in section 4 we describe how this effect determines the energy density and pressure of the instanton ensemble. A general treatment of the new interaction induced by the presence of molecules is given in section 6 while in section 7 we present the results of a simulation of a mixed ensemble of random instantons and molecules.

2 Correlations in the instanton ensemble

Let us introduce the necessary general formulae and notations. The ensemble of interacting instantons is described by a partition function of the type

$$Z = \sum_{N_+ N_-} \frac{1}{N_+! N_-!} \int \prod_i^{N_+ + N_-} [d\Omega_i d(\rho_i) \rho_i^{N_f}] \exp(-S_{int}) \prod_f^{N_f} \det(\hat{D} + m_f) \quad (1)$$

where N_+ and N_- are the numbers of instantons and anti-instantons, $d\Omega_i$ is the measure in the space of collective coordinates (12 per instanton in $SU(3)$) and

$$d(\rho) = C_{N_c} \rho^{-5} \left(\frac{8\pi^2}{g(\rho)^2} \right)^{2N_c} \exp\left(-\frac{8\pi^2}{g(\rho)^2}\right) \quad (2)$$

$$C_{N_c} = \frac{4.6 \exp(-1.86 N_c)}{\pi^2 (N_c - 1)! (N_c - 2)!} \quad (3)$$

is the semiclassical amplitude for a single instanton which depends on the running coupling constant $g(\rho)$. Furthermore, S_{int} is the gluon-induced interaction, which we do not specify in this work. Instead, we focus on the last factor, which appears after the integration over fermions has been carried out. As is the case for the bosonic zero modes, the integral over the fermion zero modes has to be performed exactly. Assuming that the fermion

determinant factorizes in a zero mode and a nonzero mode factor, the first factor is given by $\det(TT^\dagger + m_f^2)$, whereas the second factor is taken into account to gaussian order. The matrix $T_{I\bar{I}}$ is the $N/2 \times N/2$ 'hopping' matrix

$$T_{I\bar{I}} = \int d^4x \phi_{I0}^\dagger(x - z_{\bar{I}}) i\hat{D}_x \phi_{I0}(x - z_I). \quad (4)$$

Here, $z_I, z_{\bar{I}}$ are the centers of the instantons and for simplicity we assume that², $N_+ = N_- = N/2$. The statistical mechanics described by the partition function (1) is complicated and so far direct simulations have only been carried out at zero temperature.

The instanton solutions and the corresponding zero modes are known analytically for non-zero temperature [19], and detailed studies of the temperature dependence of the 'hopping' matrix elements were performed in [20, 21]. The general structure of these matrix elements is given by $T_{I\bar{I}} = u_4 f_1 + (\vec{u}\vec{r}/r) f_2$. Here, the fourvector $u_\mu = (\vec{u}, u_4)$ is defined by $U_{I\bar{I}} = u_\mu \tau_\mu^+$, where $U_{I\bar{I}}$ is the upper 2×2 corner of the $N_c \times N_c$ matrix that describes the relative orientation of the instanton and the anti-instanton and $\tau_\mu^+ = (\vec{\tau}, -i)$. The two invariant functions f_1 and f_2 can be parameterized in the form [20]

$$f_1 = i \frac{\pi T \sin(\pi\tau T) \cosh(\pi r T)}{(\cosh(\pi r T) - \cos(\pi\tau T) + \kappa_1^2(T))^2} \cdot F_1(\tau, r, T), \quad (5)$$

$$f_2 = i \frac{\pi T \cos(\pi\tau T) \sinh(\pi r T)}{(\cosh(\pi r T) - \cos(\pi\tau T) + \kappa_2^2(T))^2} \cdot F_2(\tau, r, T). \quad (6)$$

where r and τ are the separation between the instanton and the anti-instanton in the spatial and time direction. All quantities are given in units of the geometric mean of the two instanton radii $\sqrt{\rho_I \rho_A}$. The functions F_1, F_2 and κ_1, κ_2 provide the correct normalization in the limits of zero and infinite temperature. They are explicitly specified in [20] and used in our simulations but their detailed structure is not important for the purpose of our arguments.

Neglecting all interactions one arrives at a random ensemble of instantons in which the distribution over all collective coordinates such as positions and orientation is given by the corresponding invariant measure. As was mentioned in the introduction, this model leads to a simple and phenomenologically successful description of the QCD vacuum.

²Recall that any condition applied to a macroscopically large system should not be important anyway.

Notable exceptions are those channels in which instantons produce a strong repulsion, in particular the η' and δ (scalar-isovector) channels.

Correlations in the instanton liquid have two aspects, which we will refer to as long and short range correlations. Long range correlations are related to the phenomenon of screening of the topological charge. Its most important manifestation is the vanishing of the global topological charge (and the vanishing of the topological susceptibility), which takes place provided the theory has massless fermions and one is considering a sufficiently large volume. As expressed by the Witten-Veneziano relation, these correlations are related to the physics of η' meson. We plan to discuss this question in a separate publication [22].

In the present work we want to focus on short range correlations, which can be studied by considering $I\bar{I}$ pairs. Correlations in the instanton liquid that may lead to the formation of $I\bar{I}$ pairs are caused by the gluonic action S_{int} or the effective fermion action $S_f = N_f \text{Tr} \log(\hat{D})$. Naturally, their relative role depends strongly on the number of light flavors N_f in the theory. However, both types of interaction favor the same relative orientation of the instanton and the anti-instanton. This orientation is most simply described in terms of an angle θ defined by

$$\cos(\theta) = \frac{|u \cdot R|}{|u| \sqrt{R^2}} \quad (7)$$

where $R_\mu = (\vec{r}, \tau)$ is the vector connecting the centers of the instantons and u_μ is the relative orientation vector introduced above. Maximal attraction, for both the gluon and the fermion interaction, corresponds to $\theta = 0$.

Since the probability of a given configuration is proportional to the value of the fermion determinant, configurations with a large determinant should be preferred. For a single $I\bar{I}$ pair we have $\det(\hat{D}) \sim (\cos \theta)^{2N_f}$. If this $I\bar{I}$ pair sits in the vicinity of $\theta = 0$ we will refer to it as a 'molecule'. Clearly, it maximizes the fermion determinant, or minimizes the corresponding 'energy', $-\log(\det \hat{D})$.

However, dealing with a statistical system one should not simply minimize the energy, but rather take into account the competition between minimizing the energy and maxi-

mizing the entropy (i.e. minimize the free energy). In other words, we have to determine the relative weight of the most attractive (molecular) orientation relative to all others in the $SU(3)$ group from summing over all states in the partition sum.

Before we consider this problem, let us make a brief digression. Even if the contributions of 'molecules' in the QCD vacuum is not large, there are external parameters that can increase their role. One way of doing this is to consider QCD-like theories with an increasing number of light flavors N_f . As the fermion determinant is raised to a higher power N_f , the role of correlations induced by the determinant certainly increases. Thus, one may anticipate the existence of some critical number of flavors $N_{f,cr}$ above which the instanton ensemble is dominated by molecules [23, 5]. In this paper, however, we want to consider another external parameter that has a significant effect on correlations in the instanton liquid, namely the temperature.

3 Polarization of the $I\bar{I}$ molecules

In reference [13] a schematic model was developed in order to deal with the complicated statistical mechanics described by the partition function (1). In this model the instanton ensemble is described as a mixture of a molecular and a random component. The differential activities for the two components are assumed to be

$$dZ_m = C^2 d\rho_1 d\rho_2 d^4 R dU (\rho_1 \rho_2)^{b-5} \exp \left[-\kappa(\rho_1^2 + \rho_2^2)(\overline{\rho_a^2} n_a + 2\overline{\rho_m^2} n_m) \right] \langle (T_{I\bar{I}} T_{I\bar{I}}^*)^{N_f} \rangle \quad (8)$$

for the molecular component and

$$dZ_a = 2C d\rho d^4 R dU \rho^{b-5} \exp \left[-\kappa \rho^2 (\overline{\rho_a^2} n_a + 2\overline{\rho_m^2} n_m) \right] \left\langle \frac{1}{N} \text{Tr} T T^\dagger \right\rangle^{N_f/2} \quad (9)$$

for the atomic component. Here, n_a, n_m denote the densities of the random and the molecular components, $\overline{\rho_a^2}, \overline{\rho_m^2}$ are the average square radii of instantons in the two components, C is the normalization of the single instanton density (see (2)) and $b = \frac{11}{3}N_c - \frac{2}{3}N_f$ is the coefficient of the Gell-Mann-Low function.

The model uses a simplified gluonic interaction corresponding to an average repulsion $\langle S_{int} \rangle = \kappa \rho_1^2 \rho_2^2$ parameterized in terms of a single dimensionless constant κ . The

fermion determinant for the random component is approximated by $\langle \frac{1}{N} \text{Tr} T T^\dagger \rangle^{N_f/2}$ where the average is over all positions and orientations. For the molecular component, on the other hand, the overlap matrix element is first raised to the N_f power and then averaged $\langle (T_{I\bar{I}} T_{\bar{I}I}^\dagger)^{N_f} \rangle$. This average is only performed over positions, whereas the relative orientation is kept fixed.

Using the overlap matrix elements defined in the last section, one finds a very specific temperature dependence of the quark induced interaction. The average determinant for the random component gradually decreases with temperature, whereas the determinant for the molecular component first increases (at $T \sim T_c$) and eventually, at larger T , starts to decrease. This behavior leads to the disappearance of random instantons at high temperatures and to a phase transition to a purely molecular phase in which chiral symmetry is restored.

As we are going to show in this section, the reason for this temperature dependence is given by a strong and rapid polarization of the molecules in the critical region. Polarization in this context means that at finite T the vector connecting the centers of the instanton and anti-instanton $R_\mu = z_{\bar{I}\mu} - z_{I\mu} = (\vec{r}, \tau)$ is no longer distributed isotropically (as it is at $T = 0$), but tends to point in the time direction. Roughly speaking one may say that at $T \sim T_c$ the “instanton liquid” actually becomes a “liquid crystal” of the nematic type.

In general, the anisotropy of a field theory at finite temperature is of course a consequence of the different boundary conditions imposed in the time and spatial directions. An important consequence of these boundary conditions is the fact that the propagators for bosons and fermions become qualitatively different at finite temperatures. Both are anisotropic, but fermions are subject to a qualitatively new phenomenon, the exponential screening of the propagator in the spatial direction. For a free massless fermion, the propagator is $S(r) \sim \exp(-\pi T r)$ where πT is the lowest Matsubara frequency. Therefore, with increasing temperatures quarks develop a strong preference to propagate in the time direction. This is the main mechanism that produces an anisotropy of the instanton ensemble at finite temperature ³.

³The gluonic $I\bar{I}$ interaction at finite T was studied in [20], with the result that it remains approximately

Before we come to quantitative results, let us give a qualitative explanation why the phenomenon takes place. Suppose the vector connecting the I and \bar{I} centers is $R_\mu = (\vec{r}, \tau)$. Using the overlap matrix elements specified above, the probability to have such a molecule is roughly proportional to

$$\det(i\hat{D}) \sim |\sin(\pi T\tau)/\cosh(\pi Tr)|^{2N_f}. \quad (10)$$

This factor is maximal⁴ for $r = 0$ and $\tau = \beta/2 = (1/2T)$, which is the most symmetric position of the $I\bar{I}$ pair on the torus. Note that it corresponds to a molecule polarized in the time direction. As a function of temperature one may expect the strongest effects to occur when the temperature is such that the period of the torus in the direction is about twice the typical size of a molecule. In the euclidean formalism, the phase transition becomes a simple geometric effect: the transition occurs when the $I\bar{I}$ molecules optimally fit into the 'temperature box'.

In order to study this effect in more detail we have performed a simulation of the partition function (1) for a single $I\bar{I}$ pair at finite temperature T . The interaction is given by the fermion determinant discussed in section 2 and the gluonic interaction specified in [20]. The simulation is based on a simple Metropolis algorithm in which a new random configuration of the $I\bar{I}$ pair is accepted with a probability $p \sim \exp(-S_{eff})$, where the effective action is the sum of the gluonic and fermionic parts, $S_{eff} = S_{int} + \log(\det \hat{D})$. Since there is only one pair present in our simulation we keep the size of the instantons fixed while the positions and orientations are updated.

In order to characterize the orientation of the $I\bar{I}$ molecule we introduce the angle α between the vector R_μ (connecting the I and \bar{I} centers) and the (3-d) spacelike plane: $\tan \alpha = R_0/|\vec{R}| = \tau/r$. The distribution of the polarization is then determined by averaging the α over a large number of configurations. In fig. 1 we show the differential distribution of the angle α for different temperatures and two different cases: (i) two light and one heavy flavor (QCD); and (ii) four light flavors. The distributions are normalized

⁴Note also, that near the maximum $\det(i\hat{D}) \sim \exp[-N_f\pi^2T^2(\delta\tau^2 + \delta r^2)]$, so at large number of flavors one can use a saddle point method to evaluate the contribution of this region.

to the isotropic 4-d distribution, which means they are divided by the relevant Jacobian $\cos^2 \alpha$. In both cases we observe that the distribution is practically flat (=isotropic) at low temperatures $T < 100$ MeV, but becomes strongly peaked at $\alpha = \pi/2$ for larger T . At very large temperatures, this peak starts to disappear: this happens because at high T the time dimension is so strongly squeezed that no molecules can be oriented this way. As expected, the polarization is stronger in the case of four light flavors.

In fig. 2 we show fraction of molecules in the ensemble with $|\vec{R}| < \min(R_0, 1/T - R_0)$. We observe that the degree of polarization jumps to a very large value $\simeq 70\%$ over a fairly small temperature interval $T \simeq (120 - 150)$ MeV.

Finally, let us make a comment on the physical meaning of the polarization phenomenon in a less technical language. The $I\bar{I}$ molecules are virtual (or failed) tunneling events, in which the gauge fields penetrate into a new classical vacuum only for a short period of time, and then return back. For that reason, they do not contribute to the quark condensate and other related quantities. “Polarization” of the $I\bar{I}$ molecules at $T \sim T_c$ means that at such temperatures the tunneling is concentrated in the vicinity of the same spatial point.

4 Magnetic versus electric fields, and the equation of state

Lattice data on the thermodynamics of the chiral phase transition suggest that the pressure $p(T)$ remains relatively small around the transition region, while the energy density $\epsilon(T)$ changes by about an order of magnitude over a small⁵ interval $\delta T \ll T_c$. A parametrization of the data obtained by Kogut et al. [24] together with a general discussion can be found in [25]. These authors stress that at chiral restoration $T \sim T_c$ not only the (relatively small) quark related energy and pressure are significantly changed, but that the (much larger) gluonic energy and pressure should also be modified.

⁵ For three and more massless quarks the transition is believed to be of first order, but the phenomenon mentioned above is also observed for two massless quarks (when there is a second order phase transition) and for light but massive quarks, when there is no strict phase transition at all.

Let us mention one more point emphasized in [25]: there seems to be a contradiction between the small transition temperatures $T_c \simeq 140$ MeV seen in unquenched lattice simulations and the large value of the phenomenological bag pressure $B \simeq 500$ MeV/fm³ derived from the trace anomaly [14, 26] (at $T=0$). With the usual bag model equation of state, in which the pressure at $T > T_c$ is written as the sum of the Stefan Boltzmann contribution for an ideal quark-gluon gas minus the nonperturbative bag pressure, one is unable to get a positive pressure at such a low transition temperature! The natural alternative is to assume that the nonperturbative phenomena responsible for the bag pressure at $T = 0$ are partially present at $T > T_c$ as well, so that only part of this large B is removed across the transition region.

The question whether the rearrangement of the instanton ensemble into a molecular phase can explain this behavior was studied in [13], where the schematic partition function defined by (8,9) was used to determine the instanton related contribution to the equation of state. It was indeed found that instantons give a sizeable contribution to the energy density and pressure, that the two quantities behave quite differently and that the results are roughly consistent with the lattice data. In particular, it was shown that, (i) $p_{inst}(T)$ jumps down, to about half of its value at zero temperature, while, (ii) $\epsilon_{inst}(T)$ jumps up, thus contributing to the “latent heat” of the transition.

The reason for this behavior was attributed to the specific temperature dependence of the fermion interaction used in that model. In the last section we have explained that this T -dependence is caused by the polarization of $I\bar{I}$ molecules. Now we want to show, that this phenomenon leads to a simple microscopic explanation of the energy density and pressure, related to the (color) electric and magnetic fields associated with polarized molecules.

Let us first recall some well known facts about instantons at $T = 0$. The instanton (anti-instanton) fields are selfdual (or anti-selfdual), $G_{\mu\nu} = \pm \frac{1}{2}\epsilon_{\mu\nu\alpha\beta}G_{\alpha\beta}$. In Minkowski space they correspond to classically forbidden paths and the electric and magnetic fields are related by $E_k(x) = \pm iB_k(x)$. As a consequence, in the classical energy density $\epsilon_{cl} =$

$(1/2)(E^2 + B^2)$ the negative electric term is exactly compensated by the positive magnetic one, so the configuration may be created 'out of nothing', in agreement with the classical equations of motion.

Furthermore, instantons contribute to the energy density of the QCD vacuum, but this happens not at the classical but at the quantum (one-loop) level. This is quite natural, since instantons correspond to tunneling phenomena, which are known to lower the ground state energy. In QCD, this fact can be expressed in terms of the 'stress tensor anomaly'

$$\epsilon = -\frac{b}{128\pi^2} \langle (gG)^2 \rangle \quad (11)$$

which is non-zero for the instanton solution. Here, $b = (11/3)N_c - (2/3)N_f$ is the first coefficient of the beta function. For a dilute ensemble, one can directly relate the energy density to the instanton density $\epsilon = -\frac{b}{4}n_{inst}$ [27]. As we already emphasized above, this energy is numerically rather large.

At finite instanton density (and especially in strongly correlated molecules) the fields are not purely self-dual. However, at $T = 0$ molecules are unpolarized: therefore only Lorentz scalars can have non zero vacuum expectation values. Since the liquid is relatively dilute, these deviations from self-duality just lead to a relatively small correction to the right hand side of the anomaly equation.

At finite temperature, instantons contribute to the equation of state in two ways. First, the instanton density will change, leading to a change in the bag pressure. Second, the polarization of $I\bar{I}$ molecules in the time direction causes the expectation values of the electric and magnetic fields to be different. While the first effect gives equal but opposite contributions to the energy density and pressure, non-selfdual fields give a positive contribution to both the energy density and the pressure.

In order to study this effect, we have calculated the color fields for a single molecule with given polarization. Since $I\bar{I}$ configurations are not exact solutions of the euclidean equations of motion the quantitative result depends on the specific ansatz for the gauge fields. Here we show the two most widely used forms of the gauge potential, the sum

ansatz [27] (full lines in figs. 3 and 4) and the ratio ansatz [4] (dashed lines in figs. 3 and 4).

In fig. 3 we show the modification of the action $S_{int} = S_{tot} - 2S_0$ and the energy for a single molecule polarized in the time direction at a temperature of 200 MeV. Results are given for the most attractive and the most repulsive orientation. Indeed, one finds considerable attraction for the favored orientation $\cos\theta = 1$. This interaction is weaker in the ratio ansatz, but the qualitative features are the same as in the sum ansatz. The new result is the lower panel, showing the polarization of the fields in the euclidean time direction. Both in the sum and in the ratio ansatz cases, the fields are dominantly magnetic and give a positive contribution to the classical euclidean energy density $\epsilon = 1/2\langle(B^2 - E^2)\rangle$. The effect is on the order of 15% in the sum ansatz, whereas in the ratio ansatz it is roughly 10%.

In fig. 4 we show the same calculation for a molecule which is oriented along a spacelike direction. Again we observe attraction for $\cos\theta = 1$, but this attraction is considerably weaker as compared to a polarized molecule. Also, in the ratio ansatz the molecule is now essentially self dual, while in the sum ansatz it is actually dominantly electric.

Let us now come back to the discussion of the energy density and pressure

$$\epsilon = \frac{1}{2}\langle B^2 - E^2 \rangle - g^2 \frac{b}{128\pi^2} \langle E^2 + B^2 \rangle, \quad (12)$$

$$p = \frac{1}{6}\langle B^2 - E^2 \rangle + g^2 \frac{b}{128\pi^2} \langle E^2 + B^2 \rangle. \quad (13)$$

The important point is that although $\langle E^2 + B^2 \rangle$ is much larger than $\langle B^2 - E^2 \rangle$, the former quantity is suppressed by a smaller coefficient. Therefore, even a moderate deviation from selfduality leads to a substantial contribution to the energy density and pressure! Taking $\langle B^2 - E^2 \rangle / \langle B^2 + E^2 \rangle \simeq 10\%$ from the calculation of a single molecule, one can get $\epsilon \simeq 225 \text{ MeV}/\text{fm}^3$ even if the density of instantons does not change across the transition. Thus it appears that the observed jump in the energy density can be explained by a change in the (instanton related) bag pressure plus the contribution from instanton interactions and the perturbative Stefan Boltzmann part.

5 Quark interactions induced by $I\bar{I}$ molecules

Instantons give a very successful phenomenology of the QCD vacuum, because they provide a mechanism for chiral symmetry breaking and generate strong (and quite specific) interactions between light quarks. Although instantons do not lead to confinement the interactions are able to bind quarks into mesons and baryons and lead to a quantitative description of the observed spin splittings. At the one-instanton level the interaction is described by the famous 't Hooft effective interaction [28]

$$\mathcal{L} \sim \prod_f (\bar{\psi}\phi_0)(\bar{\phi}_0\psi) \quad (14)$$

where ψ are quark operators and ϕ_0 is the zero mode wave function. The product runs over the light quark flavors. This is still a complicated nonlocal interaction which depends on the color orientation of the instanton. After taking the long wavelength limit and averaging over the color orientation it can be reduced to a local $2N_f$ -point interaction [29, 30]. In the case of two light flavors it reads

$$\mathcal{L} = \int n(\rho)d\rho \frac{(2\pi\rho)^4}{8(N_c^2 - 1)} \left\{ \frac{2N_c - 1}{2N_c} [(\bar{\psi}\tau_a^-\psi)^2 + (\bar{\psi}\tau_a^-\gamma_5\psi)^2] - \frac{1}{4N_c}(\bar{\psi}\tau_a^-\sigma_{\mu\nu}\psi)^2 \right\}, \quad (15)$$

where $n(\rho)$ denotes the density of instantons. Here, ψ is an isodoublet of quark fields and the four vector τ_a^- has components $(\vec{\tau}, i)$ with $\vec{\tau}$ equal to the Pauli matrices acting in isospace. The Dirac matrix $\sigma_{\mu\nu}$ is defined by $\sigma_{\mu\nu} = \frac{i}{2}[\gamma_\mu, \gamma_\nu]$. The interaction (15) successfully explains many properties of the ($T=0$) QCD correlation functions, most importantly the strong attraction seen in the pion channel.

At finite temperature the collective coordinates of instantons are no longer random, but become correlated. Therefore, it is no longer possible to average over the instanton orientations and use the effective Lagrangian (15). However, due to the presence of molecule there should be strong non-perturbative effects even around T_c s. For this reason we would like to investigate what kind of interactions are induced by correlated $I\bar{I}$ pairs. We first study the quark propagator in the field of an instanton anti-instanton molecule and then derive the effective vertex that reproduces all four quark correlations.

The quark propagator in the field of a single molecule is given by

$$S_{ij}^{ab}(x, y) = S_0(x, y) + \frac{1}{T_{I\bar{I}}} \left(\phi_{I,i}^a(x) \phi_{I,j}^{b\dagger}(y) + \phi_{I,i}^a(x) \phi_{I,j}^{b\dagger}(y) \right). \quad (16)$$

Here ϕ_I and $\phi_{\bar{I}}$ denote the zero mode wavefunctions in the field of the instanton and the anti-instanton and $T_{I\bar{I}}$ is the corresponding overlap matrix element. For simplicity we use the zero temperature profiles. We neglect all non-zero mode contributions except for the free propagator S_0 . The propagator (16) satisfies the following symmetry relation

$$S^\dagger(x, y) = S(y, x). \quad (17)$$

For $N_c = 2$ the symmetry group is larger. In that case we can relate the propagator to its transpose by

$$S(x, y) = -\sigma_2 \gamma_5 C S^T(y, x) C \gamma_5 \sigma_2 \quad (18)$$

which is also known as the Pauli-Gürsey symmetry [31]. The Pauli matrix σ_2 acts in color space. A remnant of this symmetry is still present for more than two colors. If we remember that correlators of color singlet currents only depend on the relative $I\bar{I}$ orientation, which in the case of molecules is given by $R_\mu \tau_\mu^+$, it is clear that the symmetry (18) holds in the gauge that one of the pseudoparticles has the identity as orientation matrix. In that case σ_2 contains a projector of $SU(N_c)$ on the $SU(2)$ subgroup where the $I\bar{I}$ molecule has its support.

To investigate the consequences of the symmetries (17, 18) let us consider the tensor decomposition of the propagator

$$S^{ab}(x, y) = \sum_i a_i^{ab}(x, y) \Gamma_i, \quad (19)$$

where Γ_i is the complete set of (hermitean) Dirac matrices. Due to the chiral structure of the propagator only the vector $a_{V\mu}$ and the axial vector $a_{A\mu}$ components are non-zero. For the scalar, pseudoscalar and tensor components we have

$$a_S = a_P = a_{T\mu\nu} = 0. \quad (20)$$

As a consequence [6] the scalar and the pseudo-scalar correlator are degenerate. Also the axial and the vector correlator are degenerate, whereas the tensor correlator is not affected by the presence of molecules.

The symmetry (17) leads to the relation

$$a_i(x, y) = a_i^\dagger(y, x). \quad (21)$$

Under the restrictions quoted below (18) also the following two equalities hold

$$a_{V\mu}(x, y) = -\sigma_2 a_{V\mu}^T(y, x) \sigma_2, \quad (22)$$

$$a_{A\mu}(x, y) = \sigma_2 a_{A\mu}^T(y, x) \sigma_2, \quad (23)$$

An immediate consequence of (22) is that

$$\text{Tr}(S(x, x) \gamma_\mu) = 0. \quad (24)$$

This term enters the disconnected contribution to the isoscalar correlation function. The relation (24) therefore implies that in the molecular vacuum the rho and omega mesons are degenerate⁶. To exploit the relations (22,23) further, we remind the reader the definition of a flavor non-singlet meson correlator

$$\Pi_\Gamma^M(x, y) = \text{Tr}(S(x, y) \Gamma S(y, x) \Gamma), \quad (25)$$

and the corresponding diquark correlator

$$\Pi_\Gamma^D(x, y) = \text{Tr}(S(x, y) \Gamma C \sigma_2 S^T(x, y) \sigma_2 C \Gamma), \quad (26)$$

where we have chosen a particular color component of the diquark (every antisymmetric color matrix defines a diquark current). Again, σ_2 projects onto a $SU(2)$ subgroup of $SU(N_c)$. From (18) we conclude that meson correlators in the channel Γ are degenerate with diquark correlators in the channel $\Gamma \gamma_5$ up to a color factor. This factor is given by $2/N_c(N_c - 1)$ which counts the total number of embeddings of instantons in $SU(N_c)$.

⁶This is quite remarkable since the near-degeneracy of the rho and omega mesons has no really good explanation. In fact, finite- T QCD sum rules suggest that the degeneracy is lifted at finite T whereas our model predicts that it remains present.

For $N_c = 2$ the Pauli-Gürsey symmetry becomes exact and meson and diquarks are degenerate.

In [6] it was shown that all meson correlators can be expressed in the coefficients of the tensor decomposition of the propagator. In the molecular vacuum, the coefficients obey simple relations which allow us to find relations between the correlators. We find

$$\overline{\sum_{kl} |a_{V\mu}^{kl}(x, y)|^2} = 3 \overline{\sum_{kl} |a_{A\mu}^{kl}(x, y)|^2}, \quad (27)$$

and

$$\overline{\sum_{kl} |a_{A\mu}^{kl}(x, y)|^2} = \frac{1}{2} \overline{\sum_{kl} |a_{A\mu}^{kk}(x, x) a_{A\mu}^{ll}(y, y)|}, \quad (28)$$

where the averaging is performed over the color and spatial orientation of the molecule and we have assumed that x and y are far away from the locations of the pseudoparticles. The relation (27) determines unflavored correlation functions [6], whereas (28) gives the disconnected contribution for flavor singlet correlation functions. Note that (24) implies that $a_{V\mu}^{kl}(x, x) = 0$. If the propagator is calculated in the spatial direction, the relations (27,28) remain valid even the molecules are polarized in the temporal direction.

The effective vertex for quark-quark scattering in the molecular vacuum can be obtained using the standard reduction formula

$$\begin{aligned} \langle p_1 p_2 | \mathcal{L}_{mol} | p_3 p_4 \rangle &= - \int \prod_{i=1}^4 d^4 x_i e^{ip_1 x_1 + ip_2 x_2 - ip_3 x_3 - ip_4 x_4} \bar{\psi}_m^a(\hat{p}_1)_{mi} \bar{\psi}_n^b(\hat{p}_2)_{nj} \\ &\quad \langle 0 | T(\bar{q}_i^a(x_1) \bar{q}_j^b(x_2) q_k^c(x_3) q_l^d(x_4)) | 0 \rangle (\hat{p}_3)_{kp} \psi_p^c(\hat{p}_4)_{lq} \psi_q^d, \end{aligned} \quad (29)$$

where ψ_i^a is an isodoublet fermion field with color index a and spinor index i . If we treat the correlated instanton ensemble as a dilute gas of molecules, the vacuum expectation value can be calculated using the quark propagator (16). We only have to perform the average over the global color orientation of a molecule whereas the relative orientation between the the instanton and the anti-instanton is kept fixed. At low temperatures, molecules are unpolarized and we average over the direction of the vector connecting the centers of the instantons. After taking the long wavelength limit we obtain a local four

fermion interaction

$$\begin{aligned}
\mathcal{L}_{mol} = G & \left\{ \frac{1}{N_c(N_c - 1)} [(\bar{\psi}\gamma_\mu\psi)^2 + (\bar{\psi}\gamma_\mu\gamma_5\psi)^2] - \frac{N_c - 2}{N_c(N_c^2 - 1)} [(\bar{\psi}\gamma_\mu\psi)^2 - (\bar{\psi}\gamma_\mu\gamma_5\psi)^2] \right. \\
& + \frac{2N_c - 1}{N_c(N_c^2 - 1)} [(\bar{\psi}\tau^a\psi)^2 - (\bar{\psi}\tau^a\gamma_5\psi)^2] \\
& \left. - \frac{1}{N_c(N_c - 1)} [(\bar{\psi}\tau^a\gamma_\mu\psi)^2 + (\bar{\psi}\tau^a\gamma_\mu\gamma_5\psi)^2] \right\} \quad (30)
\end{aligned}$$

with the coupling constant

$$G = \int n(\rho_1, \rho_2) d\rho_1 d\rho_2 \frac{1}{8T_{II}^2} (2\pi\rho_1)^2 (2\pi\rho_2)^2. \quad (31)$$

Here $n(\rho_1, \rho_2)$ is the total tunneling probability for the $II\bar{I}$ pair. Note that the isospin structure of (32) is different from (15), τ^a is a fourvector with components $(\vec{\tau}, 1)$. When calculating correlation functions from this effective vertex both the direct and the exchange term have to be taken into account. In order to extract the relevant coupling in each channel directly from the Lagrangian we add the exchange term and Fierz rearrange it into an effective direct interaction. The resulting Fierz symmetric Lagrangian reads

$$\begin{aligned}
\mathcal{L}_{mol\ sym} = G & \left\{ \frac{2}{N_c^2} [(\bar{\psi}\tau^a\psi)^2 - (\bar{\psi}\tau^a\gamma_5\psi)^2] \right. \\
& \left. - \frac{1}{2N_c^2} [(\bar{\psi}\tau^a\gamma_\mu\psi)^2 + (\bar{\psi}\tau^a\gamma_\mu\gamma_5\psi)^2] + \frac{2}{N_c^2} (\bar{\psi}\gamma_\mu\gamma_5\psi)^2 \right\} + \mathcal{L}_8, \quad (32)
\end{aligned}$$

where \mathcal{L}_8 denotes the color octet part of the interaction

$$\begin{aligned}
\mathcal{L}_8 = G & \left\{ \frac{N_c - 2}{2N_c(N_c^2 - 1)} [(\bar{\psi}\tau^a\lambda^i\psi)^2 - (\bar{\psi}\tau^a\lambda^i\gamma_5\psi)^2] \right. \\
& + \frac{1}{4N_c(N_c - 1)} [(\bar{\psi}\tau^a\lambda^i\gamma_\mu\psi)^2 + (\bar{\psi}\tau^a\lambda^i\gamma_\mu\gamma_5\psi)^2] \\
& - \frac{1}{2N_c(N_c - 1)} [(\bar{\psi}\lambda^i\gamma_\mu\psi)^2 + (\bar{\psi}\lambda^i\gamma_\mu\gamma_5\psi)^2] \\
& \left. - \frac{2N_c - 1}{2N_c(N_c^2 - 1)} [(\bar{\psi}\lambda^i\gamma_\mu\psi)^2 - (\bar{\psi}\lambda^i\gamma_\mu\gamma_5\psi)^2] \right\}. \quad (33)
\end{aligned}$$

At temperatures around the critical temperature for the chiral phase transition, molecules become polarized in the time direction and we should not average over the relative position of the instanton and the anti-instanton. In this case we get an effective lagrangian which is identical to (30,33) but with all vector interactions modified according to $(\bar{\psi}\gamma_\mu\psi)^2 \rightarrow 4(\bar{\psi}\gamma_0\psi)^2$.

Like the effective interaction in the dilute instanton gas, (15), the result for the molecular vacuum is $SU(2) \times SU(2)$ symmetric. But in addition to being chirally symmetric, the effective lagrangian in the molecular vacuum is also $U(1)_A$ symmetric. Local fermion lagrangians of this type have been studied extensively in the context of the Nambu and Jona-Lasinio (NJL) model [32]. However, in contrast to the NJL model the effective interaction in the instanton model changes above the chiral phase transition. Furthermore, the NJL model has four unknown coupling constants, even when one restricts oneself to zero temperature and colour singlet terms only. At finite temperature, the number of independent couplings is even larger since the space- and timelike vector currents can have different couplings constants. In our model, all coupling constants are specified in terms of a single parameter G .

Let us now compare the 't Hooft interaction (15) (dominant at $T = 0$) and the 'molecule-induced' one we just derived, valid for $T > T_c$. The main effects of the 't Hooft interaction are (i) the strong attraction in the pion channel and (ii) the strong repulsion in the η' channel. The 'molecule-induced' effective lagrangian is also attractive in the pion channel, but (since chiral and $U(1)_A$ symmetry are restored) the same attraction also operates in the scalar-isoscalar (σ), scalar-isovector (δ) and pseudoscalar-isoscalar (η') channels.

Furthermore, this lagrangian also includes an attractive interaction in the vector and axial vector channels. If molecules are unpolarized, the corresponding coupling constant is a factor of four smaller than the scalar coupling. If they are completely polarized, the attraction is present only in the operators containing γ_0 , but becomes equally strong as the attraction in the scalar-pseudoscalar channels. Transversely polarized vectors are not affected in this case.

There are further non-trivial qualitative features of the new effective Lagrangian. Note that it predicts no splitting between the isoscalar (ω) and isovector (ρ) vector channels. As we explained above, this is a consequence of the remnant of the Pauli-Gürsey symmetry in the molecular vacuum. At the same time, there appears additional repulsion in the

axialvector-isoscalar (f_1) channel compared to axialvector-isovector (a_1) case.

In order to estimate the effective interaction in baryons we would like to start with a simpler problem and study the interaction for diquarks. The effective lagrangian (30) can be rearranged into the form

$$\begin{aligned} \mathcal{L} = G \left\{ \frac{2}{N_c^2(N_c - 1)} \left[(\bar{\psi} C \tau^A \beta^c \bar{\psi}^T)(\psi^T C \tau^A \beta^c \psi) - (\bar{\psi} \gamma_5 C \tau^A \beta^c \bar{\psi}^T)(\psi^T C \gamma_5 \tau^A \beta^c \psi^T) \right] \right. \\ \left. - \frac{1}{2N_c^2(N_c - 1)} \left[(\bar{\psi} \gamma_\mu C \tau^S \beta^c \bar{\psi}^T)(\psi^T C \gamma_\mu \tau^S \beta^c \psi) \right. \right. \\ \left. \left. - (\bar{\psi} \gamma_\mu \gamma_5 C \tau^A \beta^c \bar{\psi}^T)(\psi^T C \gamma_\mu \gamma_5 \tau^A \beta^c \psi) \right] \right\} + \mathcal{L}_6 \quad (34) \end{aligned}$$

where \mathcal{L}_6 denotes the effective interaction among color sextet diquarks. Only the anti-symmetric color matrices β^c enter in (34). In order to facilitate the comparison with the mesonic interaction [33], they are normalized according to $\text{Tr}(\beta^c \beta^{c'}) = N_c \delta^{cc'}$. Using this normalization, the strength of the interaction as compared to the free correlation function can be inferred directly by comparing the coupling constants. For diquarks, the isospin wavefunction is determined by the dirac structure [6, 33]. Here, τ^S denote the symmetric Pauli matrices and $\tau^A = \tau^2$ is the antisymmetric one.

From the effective lagrangian (34) we find an attractive interaction for scalar $\psi^T C \gamma_5 \psi$ and pseudoscalar $\psi^T C \psi$ diquarks. The interaction for vector diquarks is also attractive with a coupling constant that is a factor 4 smaller than the one in the scalar channel. All coupling constants are a factor $(N_c - 1)$ smaller than the ones in the corresponding mesonic channel. Again, this is a consequence of the remnant of the Pauli-Gürsey symmetry.

The nucleon can be thought of as consisting of an equal mixture of scalar and vector diquarks coupled to a third quark, whereas the delta resonance only contains vector diquarks. Using the effective interaction derived above, we would therefore expect an attractive interaction for the nucleon. The delta-nucleon splitting, however, is expected to be significantly smaller than the pi-rho splitting since the coupling in the diquark channel is a factor of 2 smaller than the coupling for mesons.

The most direct consequence of the Lagrangian (30) is the behavior of mesonic correlation functions. We will study this question in the next section. The corresponding

measurements on the lattice provide the relevant test in order to check the correctness of our model. Before we come to this, we would like to consider an even simpler set of physical quantities at nonzero T , the expectation values of four quark operators. These matrix elements play an important role in QCD sum rule calculations and some of them can be considered as additional order parameters for chiral symmetry breaking. It is therefore interesting to check whether they vanish at $T = T_c$ in a universal manner. At low temperatures, the temperature dependence of these expectation values can be determined by calculating the contribution from single pion states. At large temperatures $T \simeq T_c$, however, little is known about the T -dependence. Usually it is assumed that the expectation values can be factorized

$$\langle\langle \bar{q}\Gamma q \bar{q}\Gamma' q \rangle\rangle \simeq \frac{1}{(4N_c N_f)^2} (\text{Tr}(\Gamma)\text{Tr}(\Gamma') - \text{Tr}(\Gamma\Gamma')) \langle\langle \bar{q}q \rangle\rangle^2, \quad (35)$$

where the double brackets indicate thermal expectation values. This would imply that all expectation values of four quark operators are restored at T_c , and that they vanish at twice the rate of the quark condensate.

Alternative $SU(N_f)$ order parameters are given by the expectation values

$$O_1(T) = \langle\langle [\bar{u}_L \gamma_0 u_L - \bar{d}_L \gamma_0 d_L][L \rightarrow R] \rangle\rangle, \quad (36)$$

$$O_2(T) = \langle\langle [\bar{u}_L \gamma_i u_L - \bar{d}_L \gamma_i d_L][L \rightarrow R] \rangle\rangle, \quad (37)$$

$$O_3(T) = \langle\langle [\bar{u}_L \gamma_0 t^a u_L - \bar{d}_L \gamma_0 t^a d_L][L \rightarrow R] \rangle\rangle, \quad (38)$$

$$O_4(T) = \langle\langle [\bar{u}_L \gamma_i t^a u_L - \bar{d}_L \gamma_i t^a d_L][L \rightarrow R] \rangle\rangle, \quad (39)$$

where $t^a = \lambda^a/2$ are the generators of $SU(N_c)$. These operators enter the Weinberg sum rules at non-zero temperatures, related to the difference between vector and axial correlators [34]. Instead of the operators listed above, one may also consider the combinations only containing left or right handed quark fields. These operators are related to the sum of the vector and axial vector correlators, and need not be restored above the chiral phase transition.

A quantity sensitive to $U(1)_A$ violation is nothing else but the expectation value of

the 't Hooft vertex

$$O'^{tHooft}(T) = \langle\langle \det_f(\bar{q}_{f,R} q_{f,L}) \rangle\rangle, \quad (40)$$

where the determinant is taken over the different quark flavors $f = u, d, \dots$ and L, R stand for left and right components of the quark fields. Around or above T_c there is no quark condensate, and 'unpaired' instantons have very small density $O(m^{N_f})$ [28]. However, in the measurement of quantities like this one, the denominators of the quark propagators cancel the current quark masses, recovering the famous 't Hooft effective interaction. In a sense, the operator considered can induce a tunneling event by itself. Unfortunately, this implies that a small fraction of the configurations will produce a large signal. This is certainly not an easy way for measurements to be performed.

Finally, at the end of this section let us address the question of the absolute strength of the 'molecule-induced' new effective interactions. Instead of 7 unknown constants (which would appear in a general NJL-type Lagrangian for $T > T_c$) we have only G , which is determined by the number of $I\bar{I}$ molecules $n_{mol}(T)$.

Let us make a few general remarks. First, there should be a general upper bound, $n_{mol}(T) < n_c$ (the density should be smaller than some critical number for all $T > T_c$) following from the condition that the effective interaction should not be strong enough to lead to a rearrangement of the vacuum and cause spontaneous breakdown of chiral symmetry. Second, in a fully polarized configuration the interaction in the pion and longitudinal vector channel are identical. This might lead to a situation in which all scalars as well as the longitudinal components of vector and axial mesons are massless. This speculative scenario resembles the "vector limit" studied in [35].

Third, and the most natural case, is that the density of molecules and the effective interaction is simply too weak to produce any bound state. However, it can still be important and lead to observable effects: one of them being modification of the 'screening masses' to be discussed in the next section.

6 Correlation functions in the 'Cocktail Model'

Having outlined the main qualitative features of the interactions induced by $I\bar{I}$ molecules, and local averages induced by them, we now want to study more complicated predictions of this model involving various correlation functions.

For this purpose we introduce a schematic model along the lines proposed in [13]. In this model we assume that the total number of instantons at temperatures around the chiral phase transition is not much smaller than at $T = 0$. We then study the phase transition by varying the fraction $f = 2N_{mol}/N_{inst}$ of instantons correlated in $\bar{I}I$ molecules.

We have carried out our simulations in a box $5.8^3 \times 1.3 \text{ fm}^4$, corresponding to a total volume $V = 256 \text{ fm}^4$ and a temperature $T = 150 \text{ MeV}$. This is the temperature that determines the boundary conditions on the fields and enters in the calculation of the propagators. As we have explained in section 4 we consider a scenario in which the phase transition takes place over a fairly narrow interval of temperatures $\delta T \ll T_c$. Since the instanton fields vary smoothly with temperature, we keep the size of the box fixed while we vary the fraction of molecules.

The calculation of the spectrum of the Dirac operator, the quark condensates and hadronic correlation functions follows our earlier work on the random instanton model [6]. The essential idea is to exactly diagonalize the Dirac operator in the space spanned by the zero modes of the individual instantons and treat the effects of the non zero modes on the single instanton level. In this work we simply replace all the eigenfunctions and overlap matrix elements by their finite temperature counterparts. This means in particular that the quark propagator is antiperiodic in the time direction and becomes screened for large spacelike separations.

In fig. 5 we show the behavior of the quark condensate $\langle\langle\bar{q}q\rangle\rangle$ (denoted by asterixes connected by the full line) and the other vacuum expectation values introduced in section 5 as a function of the fraction f of molecules. The dashed line shows the square of the condensate. The expectation values of the 't Hooft operator $\langle\langle O'^{\text{tHooft}}\rangle\rangle$ are repre-

sented by open squares. The behavior of the four quark condensates $O_1 - O_4$ is almost indistinguishable (full squares) and we show only one of them. All matrix elements are normalized to their value at $f = 0$. One clearly observes the restoration of chiral symmetry as the fraction of molecules approaches $f = 1$. In our schematic model, not only chiral symmetry but also $U(1)_A$ symmetry is restored as $f \rightarrow 1$. This is apparent from the behavior of $\langle\langle O^{\text{tHoof}} \rangle\rangle$, which is very large in the random model but vanishes in the molecular vacuum⁷. The factorization assumption fails badly for this operator but works fairly well for the vector operators O_i .

More microscopic information is given by the spectrum of the Dirac operator which we show in fig. 6. For the purely random vacuum, the spectrum is peaked at small eigenvalues λ . Using the Casher Banks formula $\langle\bar{q}q\rangle = -n(\lambda=0)/\pi$, this behavior shows that chiral symmetry is indeed broken. In the purely molecular phase, the distribution of eigenvalues is peaked at finite λ , the density of eigenvalues at zero vanishes and chiral symmetry is restored. The position of the maximum of the eigenvalue distribution reflects the typical inverse size of the molecules. For arbitrary concentrations f we observe that the spectrum looks like a linear combination of a random and a molecular component. This means that the Dirac operator really decomposes into a random part and independent 2×2 blocks corresponding to molecules.

Further details on the restoration of chiral symmetry are provided by hadronic correlation functions. Here we will only discuss spacelike correlators, since the corresponding screening masses have received a lot of attention in lattice calculations. We will present the corresponding temporal correlators in a forthcoming publication [36]. The correlators in the pion, delta, rho and a_1 channel are shown in fig. 7 and fig. 8. As the fraction of molecules approaches unity, one clearly observes that chiral symmetry is restored and the pion and delta as well as the rho and a_1 channels become degenerate. However, this does not mean that the correlation functions become purely perturbative. While the vector channels are indeed very close to the square of a massless thermal quark propagator, the

⁷As explained in section 5, this does not preclude the possibility that the $U(1)_A$ symmetry remains broken in an unquenched calculation.

scalar meson correlation functions are significantly larger than what would be expected from the propagation of free quarks.

This is also apparent from the results for the spacelike screening masses which we show in fig. 10. If the correlation functions are dominated by the propagation of free massless quarks, the spacelike screening masses are expected to behave as $2\pi T$ for mesons and $3\pi T$ for baryons [37]. As the fraction of molecules approaches one, the screening masses for the vector mesons ρ and a_1 go to $2\pi T$ while the pion remains significantly lighter. This is consistent with the effective interaction discussed in the last section. Moreover, it is also in agreement with lattice results for the spacelike screening masses in the relevant regime $T_c \sim 2T_c$ [38].

We emphasize that the results shown in fig. 7 imply the restoration of $U(1)_A$ as well as chiral symmetry [39] since the isovector scalar (δ) meson is not the chiral partner of the pion. As was remarked in [40] this effect actually may have been observed on the lattice; the sigma meson correlation function determined in most lattice simulations is actually closer to the delta meson correlator. The reason is that the two loop graphs which distinguish the two correlation functions are difficult to measure and usually neglected in lattice simulations.

In fig. 9 we show the behavior of the nucleon and delta correlation functions. Among the various possible correlation functions we only show the chiral even correlators of the first Ioffe current for the nucleon $\eta_1 = \epsilon^{abc}(u^a C \gamma_\mu u^b) \gamma_\mu \gamma_5 d^c$ and the standard delta current $j_\mu = \epsilon^{abc}(u^a C \gamma_\mu u^b) u^c$ (Π_2^N and Π_2^Δ in the notation of [6]). The chiral odd correlators vanish as $f \rightarrow 1$, in agreement with chiral symmetry restoration. In this limit the chiral even correlators approach the cube of a thermal quark propagator. Similar to the pion channel, there is some residual interaction present in the nucleon channel. The screening mass of the delta approaches $3\pi T$ as $f \rightarrow 1$, whereas the nucleon screening mass remains somewhat smaller. However, the effect is much less pronounced as compared to the pion channel.

As a consequence of chiral symmetry restoration, the nucleon is expected to become

degenerate with its chiral partner, which is usually identified with the lightest odd parity N^* resonance. Unfortunately, there is no current that couples exclusively to the N^* and not to the nucleon so that the corresponding screening mass is difficult to determine⁸. However, the fact that the chiral odd nucleon correlation functions vanish implies that any contribution from a positive parity nucleon resonance to these correlators is exactly cancelled by the contribution of the corresponding negative parity resonance. This provides at least an indirect check for the statement that the nucleon and its chiral partner are degenerate.

7 Conclusions

In this paper we have studied various consequences of a scenario in which the chiral phase transition in QCD is described as a rearrangement of the instanton liquid, going from a random phase (at low T) to a correlated phase of polarized $I\bar{I}$ molecules at $T > T_c$. In this scenario, a significant number of instantons is present at temperatures $T = T_c \sim 2T_c$, causing a variety of nonperturbative effects.

As was shown in [13] the phase transition does not require a perturbative instanton suppression but can be triggered by the temperature dependence of the fermion determinant. Here we have demonstrated that this particular behavior is due to the temperature dependence of the fermion overlap matrix elements. At temperatures $T \simeq T_c$ these matrix elements strongly favor the appearance of polarized instanton–anti-instanton molecules. This correlated instanton configuration leads to chiral symmetry restoration.

One important effect caused by instantons is the significant contribution to the energy density and pressure of the system near the phase transition region. As demonstrated in section 4 the rapid polarization of the instanton molecules causes the energy density to jump up, while the pressure lags behind and remains practically unchanged. This behavior is consistent with lattice simulations, in which the energy density rapidly reaches (or even

⁸In lattice simulations one usually uses the fact that in staggered fermion calculations different parity components are discretized on alternating lattice sites in order to identify the odd parity component of the nucleon correlation function.

overshoots) the perturbative value whereas the pressure remains rather low until $T \simeq 2T_c$ [25]. Thus, one can say that the energy of BNL AGS and CERN SPS accelerators is now used to a significant degree in order to produce gluomagnetic fields of non-perturbative origin!

The presence of $I\bar{I}$ molecules above T_c also produces quite specific interactions between light quarks. We have derived an effective local $U(2) \times U(2)$ symmetric fermion lagrangian which describes these effects. This Lagrangian is invariant under a remnant of the Pauli-Gürsey symmetry which results in the degeneracy of the rho and omega channels. We find that there is a substantial residual attraction in the scalar-pseudoscalar meson channels even above T_c . This results is in agreement with lattice simulations, in which the presence of an attractive interaction in the scalar channel has been established from an analysis of spacelike screening masses [38] and direct measurements of the scalar susceptibility [41]. The considerably weaker interaction in the vector channel follows from the behavior of the quark number (vector) susceptibility [42, 43]. In agreement with our effective Lagrangian, lattice calculations result in a coupling constant that is four times larger in the scalar-pseudoscalar channel than in the axial-vector channel [41, 44].

We have also established the presence of molecule-induced interactions at $T \sim T_c$ from direct measurements of the correlation functions in a schematic 'cocktail' model. In this model, the correlators are determined in an instanton ensemble with a given fraction f of correlated $I\bar{I}$ pairs at temperatures around the critical temperature $T \simeq 150$ MeV. As the instanton liquid becomes completely correlated, we observe the restoration of chiral symmetry. In this limit most of the spacelike screening masses approach their perturbative values, $m = 2\pi T$ for mesons and $m = 3\pi T$ for baryons. Notable exceptions are the scalar ($\pi, \sigma, \delta, \eta'$) mesons whose screening masses are significantly smaller than $2\pi T$.

Finally, we would like to comment that the 'mixed phase' (the region $T \sim T_c$) discussed above can be observed not only in lattice simulations, but also in ongoing real experiments. In fact, it is exactly the kind of matter which is now produced and studied at the CERN SPS and Brookhaven AGS (to be complemented by future experiments at RHIC and

LHC). The collective hydrodynamic expansion can naturally test the equation of state. Peaks in the dilepton spectra should provide information on the masses of vector mesons decaying in matter, so hopefully one can check modifications of the masses of the rho, the omega and the a_1 or the splitting of longitudinal and transverse components.

8 Acknowledgements

The reported work was partially supported by the US DOE grant DE-FG-88ER40388. Most of the calculations presented in this work were performed at the NERSC at Lawrence Livermore. We have benefited from many discussions about QCD thermodynamics with G. E. Brown and V. Koch. One of us (E.S.) would also like to acknowledge fruitful discussions with E.-M. Ilgenfritz and A. Smilga.

References

- [1] C. G. Callan, R. Dashen and D. J. Gross, Phys. Rev. **D17**, 2717 (1978)
- [2] E. V. Shuryak, Nucl. Phys. **B203**, 93, 116 (1982)
- [3] D. I. Diakonov, V. Yu. Petrov, Nucl. Phys. **B272**, 457 (1986)
- [4] E. Shuryak, Nucl. Phys. **B302**, 559, 574, 599 (1988); **B319**, 521 (1989).
- [5] E. Shuryak, J.J.M.Verbaarschot, Nucl. Phys. **B341**, 1 (1990).
- [6] E. Shuryak, J. Verbaarschot, Nucl. Phys. **B410**, 55 (1993); T. Schäfer, E. V. Shuryak, J. J. M. Verbaarschot, Nucl. Phys. **B412**, 143 (1994)
- [7] T. Schäfer, E. V. Shuryak, Phys. Rev. **D**, in print
- [8] E. V. Shuryak, Rev. Mod. Phys. **65**, 1 (1993)
- [9] M. C. Chu, J. M. Grandy, S. Huang, J. W. Negele, Phys. Rev. Lett. **70**, 225 (1993); Phys. Rev. **D 48**, 3340 (1993)

- [10] B. Berg, Phys. Lett. **B114**, 475 (1981) M. Teper, Nucl. Phys. **B20** (Proc. Suppl.), 159 (1991)
- [11] M. C. Chu, J. M. Grandy, S. Huang , J. W. Negele, preprint, MIT-CTP#2269, hep-lat/9312071, Phys. Rev. **D**, to be published
- [12] M.-E. Ilgenfritz, E. V. Shuryak, Nucl. Phys. **B319**, 511 (1989)
- [13] M.-E. Ilgenfritz, E. V. Shuryak, Phys. Lett. **B325**, 263 (1994)
- [14] E. V. Shuryak, Phys. Lett. **B79**, 135 (1978)
- [15] R. D. Pisarski, L. G. Yaffe, Phys. Lett. **B97**, 110 (1980); D. J. Gross, R. D. Pisarski, L. G. Yaffe, Rev. Mod. Phys. **53**, 43 (1981)
- [16] E. V. Shuryak, M. Velkovsky, The instanton density at finite temperature, preprint, Stony Brook, SUNY-NTG94-11, hep-ph/9403381
- [17] D. I. Diakonov, A. D. Mirlin, Phys. Lett. **B203**, 299 (1988)
- [18] M.A. Nowak, J.J.M. Verbaarschot and I. Zahed, Nucl. Phys. **B325** (1989) 581.
- [19] B. J. Harrington, H. K. Shepard, Phys. Rev. **D17**, 2122 (1978) B. Grossman, Phys. Lett. **A61**, 86 (1977)
- [20] E. Shuryak, J. J. M. Verbaarschot, Nucl. Phys. **B364**, 255 (1991)
- [21] V. Khoze and A. Yung, Z. Phys. **C50** (1991) 155.
- [22] E. V. Shuryak, J. J. M. Verbaarschot, Screening of the topological charge in a correlated instanton model, preprint, SUNY-NTG94-25
- [23] E.V. Shuryak, Phys. Lett. **193B** (1987) 319.
- [24] J. B. Kogut, D. K. Sinclair, K. C. Wang, Phys. Lett. **B263**, 101 (1991)
- [25] V. Koch, G. E. Brown, Nucl. Phys. **A560**, 345 (1993)

- [26] M. A. Shifman, A. I. Vainshtein, V. I. Zakharov, Nucl. Phys. **B 147** 385, (1979)
- [27] D. I. Diakonov, V. Yu. Petrov, Nucl. Phys. **B245**, 259 (1984)
- [28] G. 't Hooft, Phys. Rev. **14D**, 3432 (1976)
- [29] M. A. Shifman, A. I. Vainshtein, V. I. Zakharov, Nucl. Phys. **B163**, 43 (1980)
- [30] M. A. Nowak, J. J. M. Verbaarschot, I. Zahed, Nucl. Phys. **B324**, 1 (1989)
- [31] W. Pauli, Nuo. Cim. **6**, 205 (1957); F. Gürsey, Nuo. Cim. **7**, 411 (1958)
- [32] Y. Nambu, G. Jona-Lasinio, Phys. Rev. **122**, 345 (1961); V. Bernard, R. Jaffe, U.-G. Meissner, Nucl. Phys. **B308**, 753 (1988); S. Klimt, M. Lutz, U. Vogl, W. Weise, Nucl. Phys. **A516**, 429 (1990)
- [33] U. Vogl, Z. Phys. **A337**, 191 (1990); U. Vogl, W. Weise, Progr. Nucl. Part. Phys. **27**, 195 (1991)
- [34] J. Kapusta, E. V. Shuryak, Phys. Rev. **D49**, 4694 (1994)
- [35] H. Georgi, Phys. Rev. Lett. **63**, 1997 (1989); Nucl. Phys. **B331**, 311 (1990)
- [36] T. Schäfer, E. V. Shuryak, J. J. M. Verbaarschot, The effective interaction between quarks at high temperature, preprint, Stony Brook, SUNY-NTG-94-31, (1994)
- [37] V. L. Eletsky, B. L. Ioffe, Sov. J. Nucl. Phys. **48**, 384 (1988)
- [38] A. Gocksch, Phys. Rev. Lett. **67**, 1701 (1991)
- [39] R. D. Pisarski, F. Wilczek, Phys. Rev. **D29**, 338 (1984)
- [40] E. V. Shuryak, Comm. Nucl. Part. Phys. **21**, 235 (1994)
- [41] S. Gupta, Phys. Lett. **B288**, 171 (1992)
- [42] S. Gottlieb, W. Liu, D. Toussaint, R. L. Renken, L. Sugar, Phys. Rev. **D38**, 2888 (1988)

[43] T. Kunihiro, Phys. Lett. **B271**, 395 (1991)

[44] G. Boyd, S. Gupta, F. Karsch, E. Laerman, preprint, KFA-Jülich HLRZ 54-93, hep-lat/9405006

figure captions

figure 1 Distribution of the polarization angle of an instanton–anti-instanton molecule for different temperatures T [MeV]. The distributions are shown as a function of the orientation angle α introduced in the text and are normalized to a uniform distribution $\cos^2 \alpha$. The two figures show the two cases of two light and one massive flavor (QCD) and four massless flavours ($N_f = 4$).

figure 2 Degree of polarization of an instanton anti-instanton molecule as a function of the temperature. The two figures show the two cases of two light and one massive flavor (QCD) and four massless flavors ($N_f = 4$).

figure 3 Interaction and euclidean 'energy' $\langle E^2 - B^2 \rangle$ in units of the single instanton values for a molecule oriented in the timelike direction at a temperature $T = 200$ MeV. Results are given as a function of the molecule size d in units of the instanton radius $\rho = 0.35$ fm. The dashed curves represents the results for the ratio ansatz whereas the full lines show the results for the sum ansatz. The lower line of each pair is for the most attractive orientation whereas the upper line is for the most repulsive orientation.

figure 4 Interaction and euclidean 'energy' $\langle E^2 - B^2 \rangle$ in units of the single instanton values for a molecule oriented in the spacelike direction at finite temperature $T = 200$ MeV. Results are given as a function of the molecule size d in units of the instanton radius ρ . Curves as in figure 3.

figure 5 Quark condensates in the 'cocktail' model for various concentrations $f = 2N_{mol}/N_{inst}$ with the total density $n_{inst} = 0.75 \text{ fm}^{-4}$ and the temperature $T = 150$ MeV fixed. The various operators shown are defined in section 5 of the text. All expectation values are

normalized to their value at $f = 0$. The solid and dashed lines shows the behavior of the quark condensate $\langle \bar{q}q \rangle$ and the square of the condensate $\langle \bar{q}q \rangle^2$, the open squares represent the expectation value of the 't Hooft vertex, and the expectation values $\langle O_{1-4} \rangle$ are denoted by the full squares.

figure 6 Spectrum of the Dirac operator $i\hat{D}$ for various concentrations $f = 0.00, 0.50, 0.75, 0.90, 1.00$ of molecules. The density of instantons $n_{inst} = 0.75 \text{ fm}^{-4}$ and the temperature $T = 150 \text{ MeV}$ are fixed.

figure 7 Scalar meson correlation functions for various concentrations $f = 0.00, 0.50, 0.75, 0.90, 1.00$ of molecules. The density of instantons $n_{inst} = 0.75 \text{ fm}^{-4}$ and the temperature $T = 150 \text{ MeV}$ are fixed. The dashed curve shows the correlation function for massless quarks.

figure 8 Vector meson correlation functions for various concentrations $f = 0.00, 0.50, 0.75, 0.90, 1.00$ of molecules. The density of instantons $n_{inst} = 0.75 \text{ fm}^{-4}$ and the temperature $T = 150 \text{ MeV}$ are fixed. The dashed curve shows the correlation function for massless quarks.

figure 9 Nucleon and delta correlation functions for various concentrations $f = 0.00, 0.50, 0.75, 0.90, 1.00$ of molecules. The density of instantons $n_{inst} = 0.75 \text{ fm}^{-4}$ and the temperature $T = 150 \text{ MeV}$ are fixed. The dashed curve shows the correlation function for massless quarks.

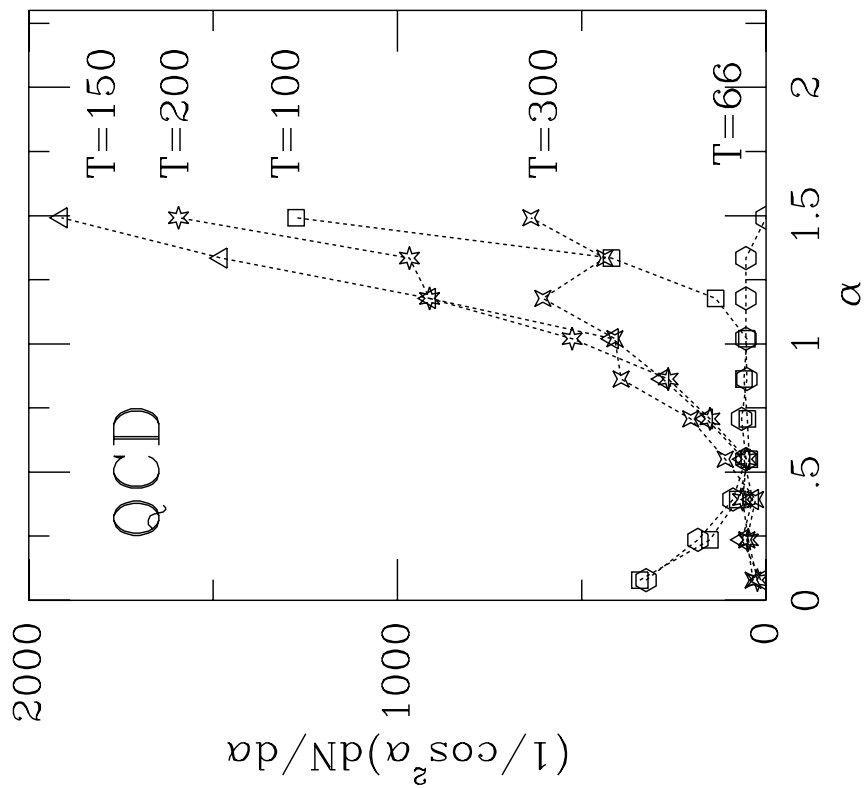
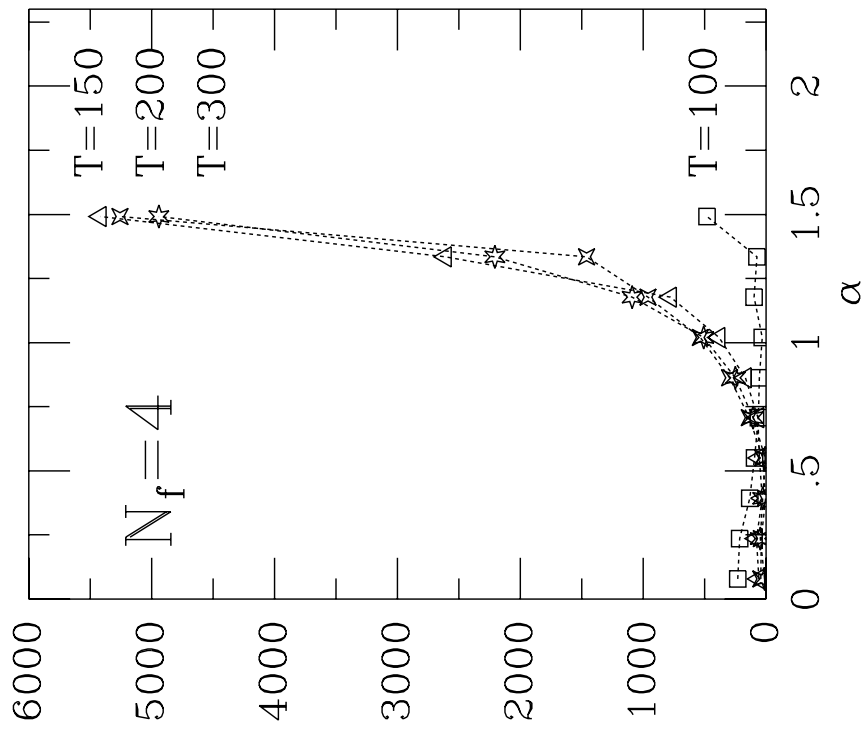
figure 10 Spacelike screening masses as a function of the concentration f of molecules. The density of instantons $n_{inst} = 0.75 \text{ fm}^{-4}$ and the temperature $T = 150 \text{ MeV}$ are fixed.

This figure "fig1-1.png" is available in "png" format from:

<http://arxiv.org/ps/hep-ph/9406210v1>

This figure "fig2-1.png" is available in "png" format from:

<http://arxiv.org/ps/hep-ph/9406210v1>



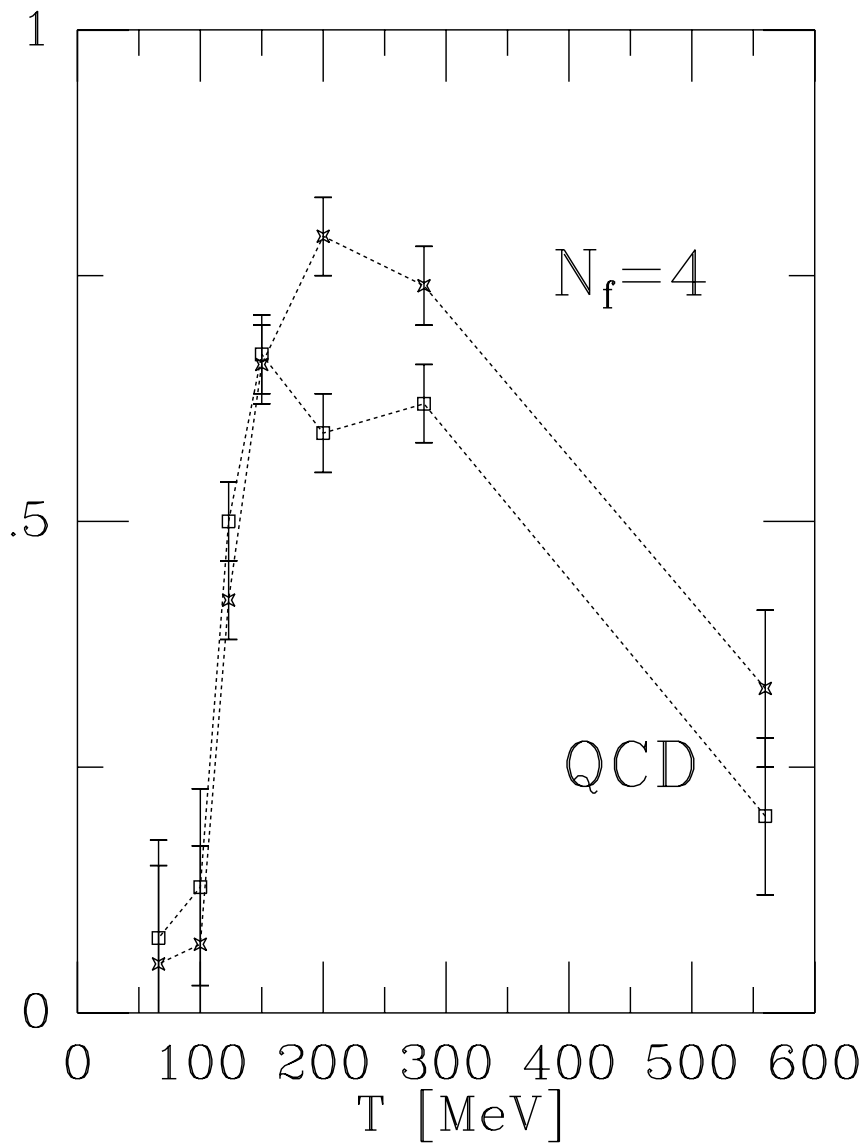
This figure "fig1-2.png" is available in "png" format from:

<http://arxiv.org/ps/hep-ph/9406210v1>

This figure "fig2-2.png" is available in "png" format from:

<http://arxiv.org/ps/hep-ph/9406210v1>

τ polarised fraction

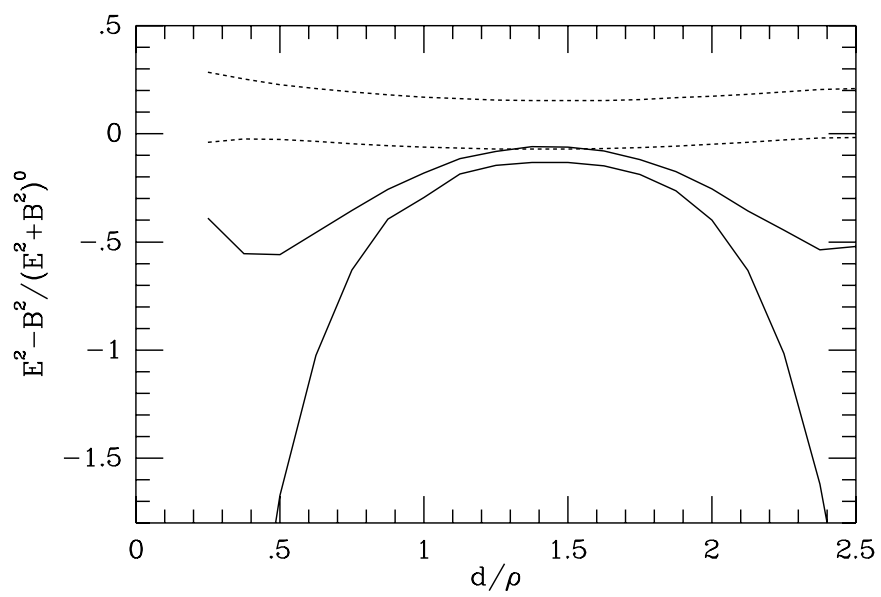
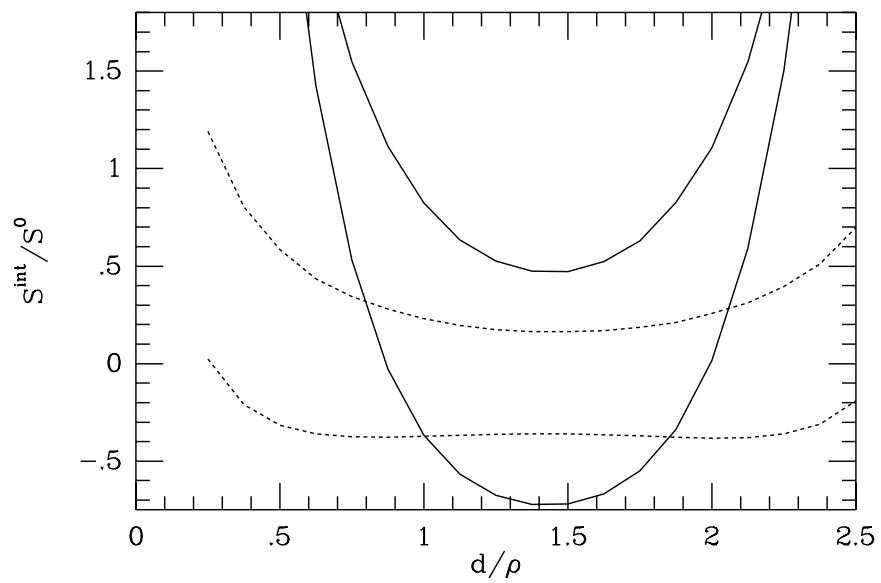


This figure "fig1-3.png" is available in "png" format from:

<http://arxiv.org/ps/hep-ph/9406210v1>

This figure "fig2-3.png" is available in "png" format from:

<http://arxiv.org/ps/hep-ph/9406210v1>

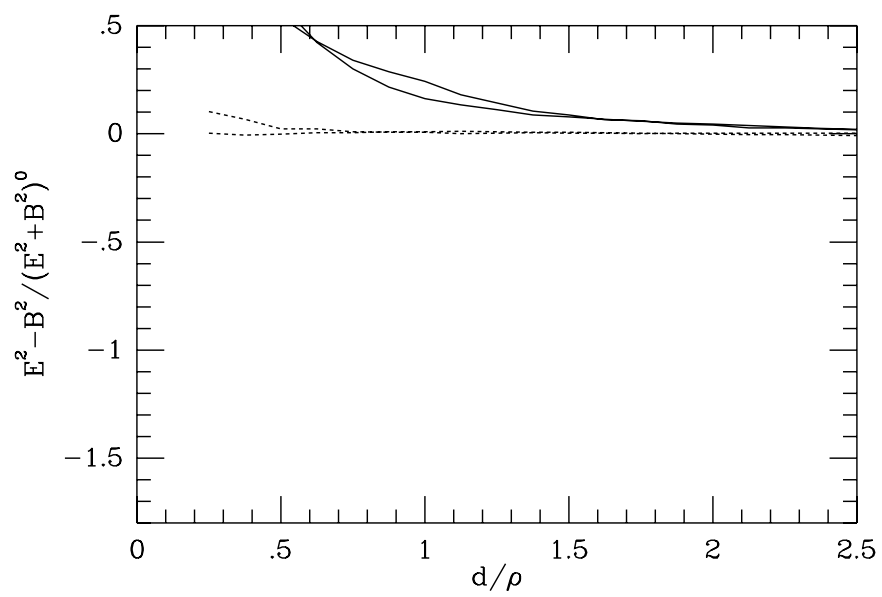
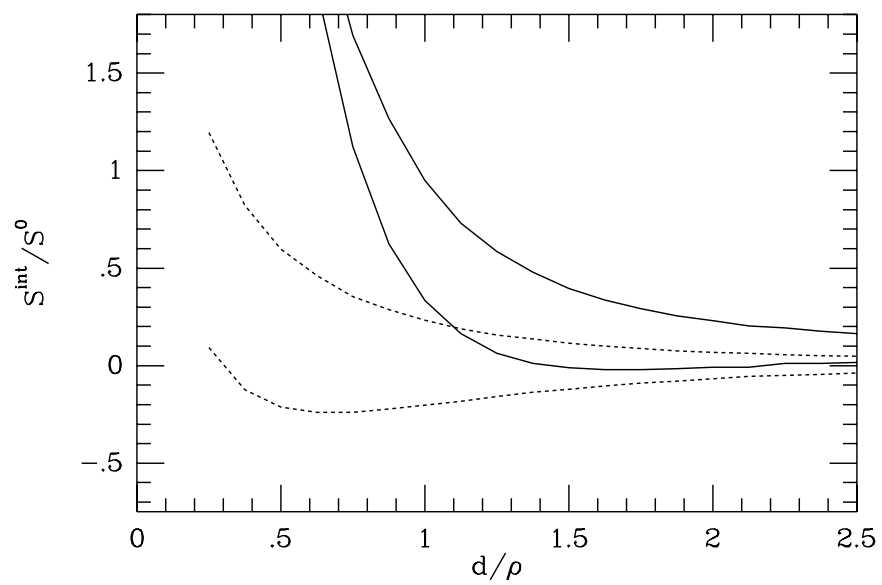


This figure "fig1-4.png" is available in "png" format from:

<http://arxiv.org/ps/hep-ph/9406210v1>

This figure "fig2-4.png" is available in "png" format from:

<http://arxiv.org/ps/hep-ph/9406210v1>



This figure "fig1-5.png" is available in "png" format from:

<http://arxiv.org/ps/hep-ph/9406210v1>

This figure "fig2-5.png" is available in "png" format from:

<http://arxiv.org/ps/hep-ph/9406210v1>

